Nuclear Magnetic Resonance Study of Atomic Motion in the Mixed Borohydride–Amide $Na_2(BH_4)(NH_2)$

ARTICLE *in* THE JOURNAL OF PHYSICAL CHEMISTRY C · JULY 2014

Impact Factor: 4.77 · DOI: 10.1021/jp503451d

6 AUTHORS, INCLUDING:

Olga Babanova
Institute of Metal Physics
16 PUBLICATIONS **152** CITATIONS
SEE PROFILE

Motoaki Matsuo
Tohoku University
74 PUBLICATIONS **912** CITATIONS
SEE PROFILE

Orimo Shin-ichi
Tohoku University
113 PUBLICATIONS **3,589** CITATIONS
SEE PROFILE

THE JOURNAL OF PHYSICAL CHEMISTRY C

Article

pubs.acs.org/JPCC

Nuclear Magnetic Resonance Study of Atomic Motion in the Mixed Borohydride–Amide $Na_2(BH_4)(NH_2)$

Alexei V. Soloninin,[†] Olga A. Babanova,[†] Evgeny Y. Medvedev,[†] Alexander V. Skripov,*[,†] Motoaki Matsuo,[‡] and Shin-ichi Orimo[‡,§]

[†]Institute of Metal Physics, Ural Division of the Russian Academy of Sciences, S. Kovalevskoi 18, Ekaterinburg 620990, Russia

[‡]Institute for Materials Research and [§]WPI-Advanced Institute for Materials Research, Tohoku University, Sendai 980-8577, Japan

ABSTRACT: To study the reorientational motion of the anions and the translational diffusion of Na^+ cations in the mixed borohydride–amide $Na_2(BH_4)(NH_2)$ showing fast-ion conduction, we have measured the ^1H, ^{11}B, and ^{23}Na NMR spectra and spin–lattice relaxation rates in this compound over broad ranges of temperature (6–480 K) and the resonance frequency (14–132.3 MHz). At low temperatures (T < 190 K), the proton spin–lattice relaxation rate is governed by fast reorientations of BH_4 groups. This reorientational process can be satisfactorily described in terms of a Gaussian distribution of the activation energies with the average E_a value of 74 ± 7 meV. Above 250 K, the measured proton spin–lattice relaxation rate originates from two other (slower) reorientational jump processes characterized by the average activation energies of 340 ± 9 meV and 559 ± 7 meV. The ^{23}Na spin–lattice relaxation data in the high-temperature region are governed by translational diffusion of Na^+ ions, which is consistent with high Na-ion conductivity in $Na_2(BH_4)(NH_2)$.

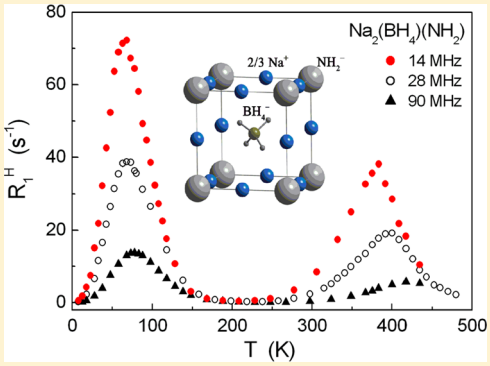

INTRODUCTION

Complex hydrides described by a general formula $M_x[AH_n]_y$, where M is a metal cation and $[AH_n]$ is a complex anion, such as $[BH_4]^-$, $[NH_2]^-$, $[AlH_4]^-$, $[NiH_4]^{4-}$, or $[SiH_3]^-$, have been attracting much recent attention as promising materials for hydrogen storage.[1] Some of these compounds were also shown to exhibit fast ionic conduction. For example, in lithium borohydride $LiBH_4$ the first-order transition from the low-T orthorhombic phase to the high-T hexagonal phase near 380 K is accompanied by the three-orders-of-magnitude increase in Li-ion conductivity, so that the conductivity exceeds 10^{-3} S/cm above 390 K.[2] Other complex hydride systems with high Li-ion conductivity include $LiBH_4$–LiX (X = Cl, Br, I) solid solutions,[3−5] $Li_2(BH_4)(NH_2)$,[6] $Li_4(BH_4)(NH_2)_3$,[6] $Li_3(NH_2)_2I$,[7] and $LiR(BH_4)_3Cl$ (R = La, Ce, Gd).[8−10] Since sodium is much more abundant and much less expensive than lithium, Na-ion conductors may provide an attractive alternative to Li-ion conductors for electrochemical applications. The recent example is $Na_2B_{12}H_{12}$ showing the extremely high Na-ion conductivity of ∼0.1 S/cm above its order–disorder phase transition at ∼520 K.[11,12]

Studies of the structural and Na-ion conductive properties of the $NaBH_4$–$NaNH_2$–NaI system[13] have revealed that the borohydride–amide $Na_2(BH_4)(NH_2)$ prepared by ball milling the 1:1 mixture of $NaBH_4$ and $NaNH_2$ exhibits the Na-ion conductivity of 2×10^{-6} S/cm at 300 K, which is several orders of magnitude higher than the conductivity of the starting materials ($NaBH_4$ and $NaNH_2$). Furthermore, $Na_2(BH_4)(NH_2)$ shows a high electrochemical stability.[13] The cubic α-$Na_2(BH_4)(NH_2)$ crystallizes in the K_3SO_4F-type structure (space group $Pm\bar{3}m$)[14,15] with two-thirds occupancy of the corresponding Na sublattice. The high concentration of vacancies in the cation sublattice is believed to facilitate ionic conductivity. Besides the α-phase of $Na_2(BH_4)(NH_2)$, the orthorhombic β modification (space group $Pbcm$) of this compound is also known.[15] However, the β phase can be formed from the α phase only after long annealing (10 days) at temperatures 340–370 K.[15] To understand the nature of high ionic conductivity in complex hydrides, it is important to study the relations between the crystal structure, anion rotational dynamics, and cation mobility. It should be noted that, for a number of borohydride-based compounds showing high Li-ion diffusivity, the fast BH_4 reorientations have also been observed. The corresponding systems include the high-temperature (hexagonal) phase of $LiBH_4$,[16,17] $LiBH_4$–LiI solid solutions,[18−20] and $LiLa(BH_4)_3Cl$.[10] While usually the anion reorientations and cation translational motion occur at different time scales, recent studies of $LiLa(BH_4)_3Cl$[10] suggest that in this compound the Li-ion jumps and a certain type of BH_4 reorientations may be correlated since they occur at the same time scale. Hydrogen dynamics and ion mobility in mixed borohydride–amide systems have not been investigated so far. Nuclear magnetic resonance (NMR) is known as the effective technique that can yield microscopic information on both reorientational motion[10,12,19,21−31] and ion diffusion[2,10,12,19,22,32,33] in borohydrides and related systems. An

Received: April 8, 2014
Revised: June 16, 2014
Published: June 23, 2014

   dx.doi.org/10.1021/jp503451d | J. Phys. Chem. C 2014, 118, 14805–14812

important advantage of NMR measurements is that different nuclei (such as ^{1}H, ^{11}B, ^{23}Na, ...) can serve as local probes of atomic motion complementing each other. The aim of the present work is to study both the reorientational motion and Na-ion diffusion in $Na_2(BH_4)(NH_2)$ using ^{1}H, ^{11}B, and ^{23}Na NMR measurements of the spectra and spin–lattice relaxation rates over wide ranges of temperature (6–480 K) and resonance frequency (14–132.3 MHz).

EXPERIMENTAL METHODS

The sample preparation was analogous to that described in ref 13. All preparation and manipulation procedures were performed in a glovebox filled with purified argon (less than 0.1 ppm of O_2). The $NaBH_4$–$NaNH_2$ mixture (1:1 molar ratio) was mechanically milled for 0.5 h in an argon atmosphere with subsequent heat treatment at 423 K for 12 h under 0.2 MPa of hydrogen using tungsten carbide balls and vial with 1:35 sample to balls mass ratio. According to X-ray diffraction analysis, the resulting sample was a single-phase cubic α-$Na_2(BH_4)(NH_2)$ compound (space group $Pm\bar{3}m$, a = 4.6909(2) Å). For NMR experiments, the sample was flame-sealed in a glass tube under vacuum.

Low-field NMR measurements were performed on a pulse spectrometer described earlier[10] at the frequencies $\omega/2\pi$ = 14, 28, and 90 MHz for ^{1}H, 28 MHz for ^{11}B, and 23 MHz for ^{23}Na. Typical values of the $\pi/2$ pulse length were 2–3 μs. The corresponding values of the rf field strength were about 20–30 G for protons and 60–90 G for ^{11}B and ^{23}Na. High-field ^{23}Na NMR measurements were performed on a Bruker AVANCE III 500 spectrometer at the frequency $\omega/2\pi$ = 132.3 MHz. The nuclear spin–lattice relaxation rates were measured using the saturation–recovery method. NMR spectra were recorded by Fourier transforming the solid echo signals (pulse sequence $\pi/2_x - t - \pi/2_y$).[34] The low-field ^{23}Na NMR spectra with the widths exceeding 100 kHz were obtained by superimposing a number of Fourier spectra excited with the magnetic field sweeping. This is a digital analogue of the Clark method[35,36] of recording broad NMR spectra.

RESULTS AND DISCUSSION

The temperature dependences of the proton spin–lattice relaxation rates measured at three resonance frequencies for $Na_2(BH_4)(NH_2)$ are shown in Figure 1. As can be seen from this figure, in the studied temperature range, the ^{1}H spin–lattice relaxation rate R_1^H exhibits two frequency-dependent peaks. Such a behavior is consistent with the coexistence of two types of atomic motion with strongly differing characteristic jump rates. For each of the peaks, the $R_1^H(T)$ maximum is expected to occur at the temperature at which the corresponding jump rate τ^{-1} becomes nearly equal to the resonance frequency ω.[37] Similar two-peak behavior of $R_1^H(T)$ has been found recently for $LiBH_4$–LiI solid solutions[19] and for $LiLa(BH_4)_3Cl$.[10]

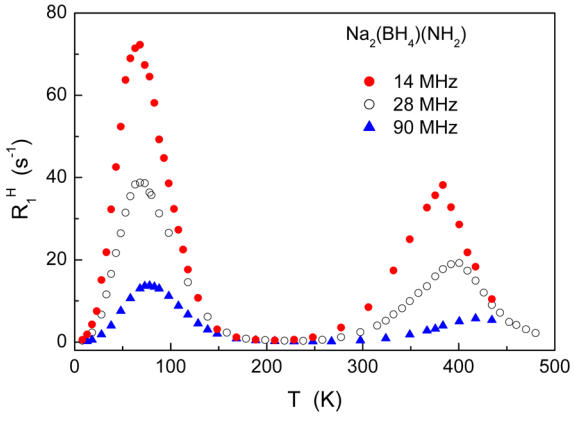

Figure 1. Temperature dependences of the proton spin–lattice relaxation rates measured at 14, 28, and 90 MHz for $Na_2(BH_4)(NH_2)$.

The low-temperature $R_1^H(T)$ peak for $Na_2(BH_4)(NH_2)$ is observed near 70 K at $\omega/2\pi$ = 14 MHz; this means that the jump process responsible for this peak is very fast (the corresponding jump rate should reach the value of $\sim 10^8$ s^{-1} already near 70 K). Comparison of these results with the $R_1^H(T)$ data for other borohydride-based systems[10,19,21–23,26] suggests that the low-T relaxation rate peak for $Na_2(BH_4)(NH_2)$ originates from reorientational motion of BH_4 groups. It is interesting to note that, as in the case of borohydride-based compounds with fast Li-ion conduction (see the Introduction), rather high Na-ion conductivity in $Na_2(BH_4)(NH_2)$[13] is accompanied by the presence of fast BH_4 reorientations. The local environment of a BH_4 group in the cubic α-$Na_2(BH_4)(NH_2)$[15] is presented in Figure 2, showing two possible orientations of the BH_4 tetrahedron that are consistent with the cubic symmetry. Each BH_4 tetrahedron is coordinated by 12 Na sites (two-thirds of which are randomly occupied by Na-ions) and 8 NH_2 groups. It is believed that the high concentration of vacancies in the Na sublattice facilitates the Na-ion conduction in $Na_2(BH_4)(NH_2)$. The NH_2 groups are shown as large gray spheres since the exact orientation of N–H bonds in them is not known.[15]

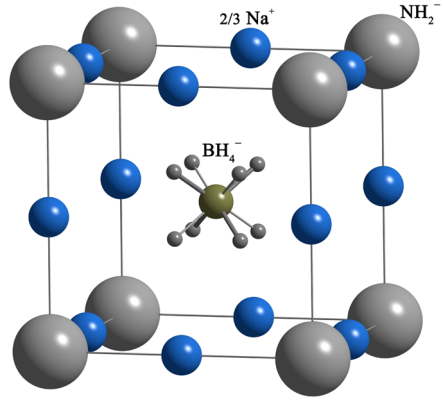

Figure 2. Local environment of a BH_4 group in the cubic α-$Na_2(BH_4)(NH_2)$. Two possible orientations of the BH_4 tetrahedron are shown. Two-thirds of the available Na sites (blue spheres) are randomly occupied by Na^+ ions. The NH_2 groups are shown as large gray spheres since the exact orientation of N–H bonds in them is not known.[15]

Figure 3 represents the evolution of the ^{1}H NMR spectrum for $Na_2(BH_4)(NH_2)$ with temperature. At low temperatures, the spectrum looks like a superposition of two lines with different widths. Such a shape is expected to originate from the presence of two H-containing groups which may have different reorientation rates. With increasing temperature, the broader component tends to disappear. The temperature dependence of the full width at half-maximum, $\Delta\nu$, of the entire measured ^{1}H NMR spectrum is shown in Figure 4. As can be seen from this figure, the motional narrowing of the spectrum occurs at very

dx.doi.org/10.1021/jp503451d | J. Phys. Chem. C 2014, 118, 14805–14812

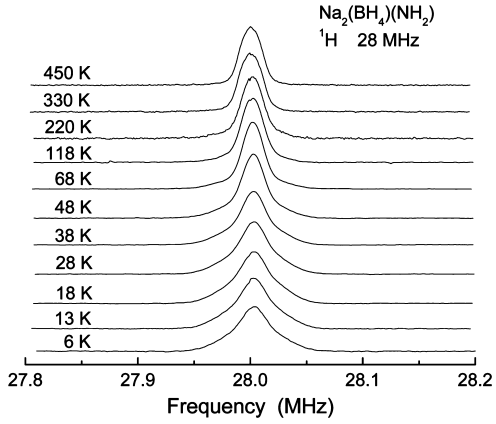

Figure 3. Evolution of the proton NMR spectrum for $Na_2(BH_4)(NH_2)$ with temperature.

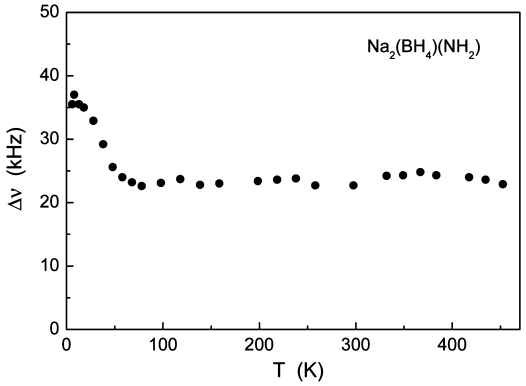

Figure 4. Temperature dependence of the width (full width at half-maximum) of the ^1H NMR line measured at 28 MHz for $Na_2(BH_4)(NH_2)$.

low temperatures (~18–50 K). At $T > 80$ K, the value of $\Delta\nu$ stops to decrease, remaining nearly constant up to the highest temperature of our measurements. The value of $\Delta\nu$ at the high-temperature plateau is rather large (~24 kHz). This is consistent with the localized nature of the H motion responsible for the observed line narrowing. Indeed, a localized motion is known to lead to only partial averaging of dipole–dipole interactions between nuclear spins.

The expected value of $\Delta\nu$ at the plateau can be roughly estimated in the following way. Since fast reorientational motion averages out the dipole–dipole interactions within the rotating group, we have to calculate only the dipole interactions between different rotating groups. Such an "intermolecular" contribution to the dipolar second moment can be estimated by placing all the nuclear spins of the group to its center and taking into account only the distances between centers of different groups.[38] Assuming a Gaussian shape of the proton NMR line, we obtain the plateau $\Delta\nu$ value of approximately 20 kHz, which is close to the experimental value of ~24 kHz for $Na_2(BH_4)(NH_2)$. In the studied temperature range, we have not found any further narrowing of the proton NMR line. Therefore, we can conclude that H-containing species do not participate in translational diffusion at the frequency scale of 10^5 s^{-1} or higher.

Low-Temperature Region. First, we discuss the behavior of the proton spin–lattice relaxation rates in the region of the low-temperature peak. The standard theory of spin–lattice relaxation due to the nuclear dipole–dipole interaction modulated by atomic motion[37] predicts that in the limit of slow motion ($\omega\tau \gg 1$) R_1^H should be proportional to $\omega^{-2}\tau^{-1}$, and in the limit of fast motion ($\omega\tau \ll 1$), R_1^H should be proportional to τ being frequency-independent. If the temperature dependence of the jump rate τ^{-1} is described by the Arrhenius law with the activation energy E_a

$$\tau^{-1} = \tau_0^{-1} \exp(-E_a/k_B T) \quad (1)$$

a plot of ln R_1^H vs T^{-1} should be linear in the limits of both slow and fast motion with the slopes $-E_a/k_B$ and E_a/k_B, respectively. Figure 5 shows the measured proton spin–lattice relaxation

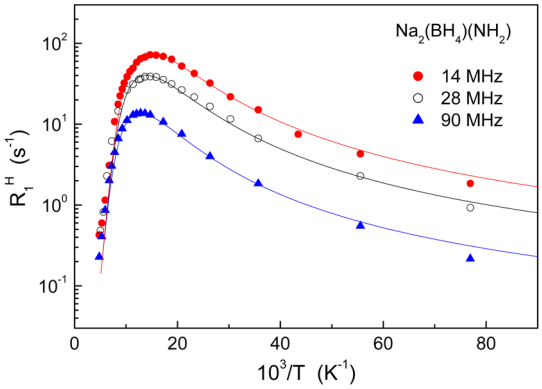

Figure 5. Proton spin–lattice relaxation rates measured at 14, 28, and 90 MHz for $Na_2(BH_4)(NH_2)$ as functions of the inverse temperature. The data are shown in the temperature range 13–209 K. The solid lines show the simultaneous fit of the model with a Gaussian distribution of the activation energies to the data.

rates in the low-T region (13–209 K) at the logarithmic scale as functions of the inverse temperature. As can be seen from Figure 5, the behavior of R_1^H in the low-T region strongly deviates from that predicted by the standard theory.

First, the observed high-temperature slope of the log R_1^H vs T^{-1} plot is much steeper than the low-temperature one; moreover, there is a pronounced curvature of the low-temperature slope. Second, the observed frequency dependence of R_1^H at the low-temperature slope is considerably weaker than the expected ω^{-2} dependence. These features are consistent with the presence of a broad distribution of H jump rates.[39] Such a distribution in $Na_2(BH_4)(NH_2)$ can be expected since Na ions in this compound randomly occupy 2/3 of 3d sites, so that the local environment of a BH_4 group (see Figure 2) changes from one group to another. The simplest approach to the description of a jump rate distribution in disordered solids is based on the model with a Gaussian distribution of the activation energies. For this model, the spin–lattice relaxation rate is expressed as[39]

$$R_1^H = \int R_1^H(E_{a1}) G(E_{a1}, \bar{E}_{a1}, \Delta E_{a1}) dE_{a1} \quad (2)$$

Here $G(E_{a1}, \bar{E}_{a1}, \Delta E_{a1})$ is a Gaussian distribution function centered at $\bar{E}_{a1}$ with the dispersion ΔE_{a1}; the subscript "1" refers to the parameters of the fast reorientational process responsible for the low-T relaxation rate peak; and $R_1^H(E_{a1})$ is given by the standard theory[37]

dx.doi.org/10.1021/jp503451d | J. Phys. Chem. C 2014, 118, 14805–14812

$$R_1^H(E_{a1}) = \frac{\Delta M_{HB1}\tau_1}{2}\left[\frac{1}{1+(\omega_H-\omega_B)^2\tau_1^2}+\frac{3}{1+\omega_H^2\tau_1^2}+\frac{6}{1+(\omega_H+\omega_B)^2\tau_1^2}\right]+\frac{4\Delta M_{HH1}\tau_1}{3}\left[\frac{1}{4+\omega_H^2\tau_1^2}+\frac{1}{1+\omega_H^2\tau_1^2}\right] \quad (3)$$

where the equation analogous to eq 1 relates the jump rate τ_1^{-1} and the corresponding activation energy E_{a1}; ω_H and ω_B are the resonance frequencies of ^{1}H and ^{11}B, respectively; and ΔM_{HB1} and ΔM_{HH1} are the parts of the dipolar second moment due to ^{1}H−^{11}B and ^{1}H−^{1}H interactions that are caused to fluctuate by the fast reorientational motion. According to our estimates, the contribution of the ^{1}H−^{23}Na dipole−dipole interaction to the proton spin−lattice relaxation rate in the low-T region can be neglected. The parameters of the model are ΔM_{HB1}, ΔM_{HH1}, τ_{01}, $\bar{E}_{a1}$, and ΔE_{a1}. These parameters have to be varied to find the best fit to the $R_1^H(T)$ data at the three resonance frequencies simultaneously. Since the H−B and H−H terms in eq 3 show nearly the same temperature and frequency dependences, it is extremely difficult to determine the amplitude parameters ΔM_{HB1} and ΔM_{HH1} independently from the fits. The estimates of the "rigid lattice" H−B and H−H contributions to the dipolar second moments in a number of borohydrides[21,23,29] suggest that ΔM_{HB1} and ΔM_{HH1} are close to each other. Therefore, for parametrization of the R_1^H data we will assume that $\Delta M_{HB1} = \Delta M_{HH1} \equiv \Delta M_1$. The solid curves in Figure 5 show the results of the simultaneous fit of the model with a Gaussian distribution of activation energies (eqs 2 and 3 and the analogue of eq 1) to the experimental data in the range 13−190 K. It can be seen that the experimental data at three resonance frequencies are satisfactorily described by a single set of parameters. The value of the amplitude parameter resulting from this fit is $\Delta M_1 = 9.2 \times 10^9$ s^{-2}, and the corresponding motional parameters are $\tau_{01} = (6.5 \pm 0.9) \times 10^{-15}$ s, $\bar{E}_{a1} = 74 \pm 7$ meV, and $\Delta E_{a1} = 29 \pm 5$ meV. It should be noted that the activation energies below 100 meV were earlier found for BH_4 reorientations in $LiBH_4$−LiI solid solutions[19,20] and $LiLa(BH_4)_3Cl$.[10]

The recovery of the ^{11}B nuclear magnetization in $Na_2(BH_4)(NH_2)$ is found to be nonexponential; it can be described by a sum of two exponential functions. The two-exponential ^{11}B relaxation was earlier observed in a number of borohydrides.[10,27] Such a behavior can be attributed[37] to the nonzero electric quadrupole moment of this nucleus. Both components of the two-exponential ^{11}B spin−lattice relaxation rate show qualitatively similar temperature dependences with two peaks. The behavior of the fast component of the ^{11}B spin−lattice relaxation rate, R_{1F}^B, is shown in Figure 6. Both R_{1F}^B peaks are observed at nearly the same temperatures as the corresponding proton spin−lattice relaxation rate peaks. This suggests that the R_{1F}^B peaks originate from the same motional processes as the corresponding R_1^H peaks.

Figure 7 shows the shape of the ^{23}Na NMR spectrum for $Na_2(BH_4)(NH_2)$ measured at $T = 90$ K and $\omega/2\pi = 23$ MHz. The shape of this spectrum is a typical example of the second-order quadrupole splitting of the central NMR line[40] in a powder sample. Such a shape indicates that there is a large static component of the electric field gradient (EFG) at Na sites, and this component is not averaged out by the fast reorientational motion of the BH_4 groups. In principle, this

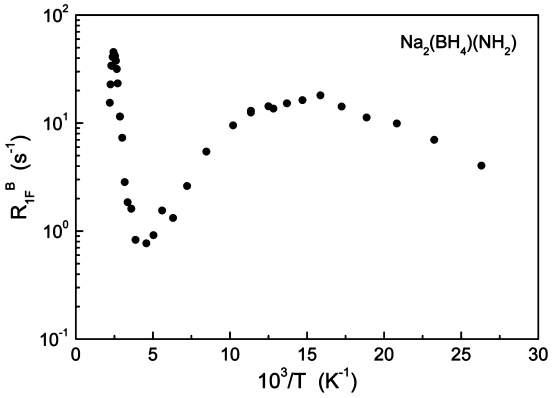

Figure 6. Fast component of the ^{11}B spin−lattice relaxation rate measured at 28 MHz for $Na_2(BH_4)(NH_2)$ as a function of the inverse temperature. The data are shown in the temperature range 38−453 K.

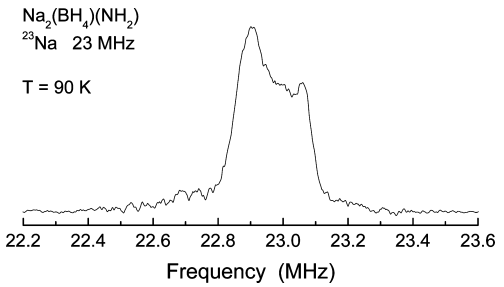

Figure 7. ^{23}Na NMR spectrum for $Na_2(BH_4)(NH_2)$ measured at 23 MHz and 90 K.

shape is consistent with the axial local symmetry of Na sites in $Na_2(BH_4)(NH_2)$ (see Figure 2). The value of the nuclear quadrupole frequency ν_Q estimated from the splitting[40] is 3.1 MHz. The fluctuating part of EFG at Na sites due to the BH_4 reorientations appears to be considerable as well. This is supported by the results of the ^{23}Na spin−lattice relaxation rate

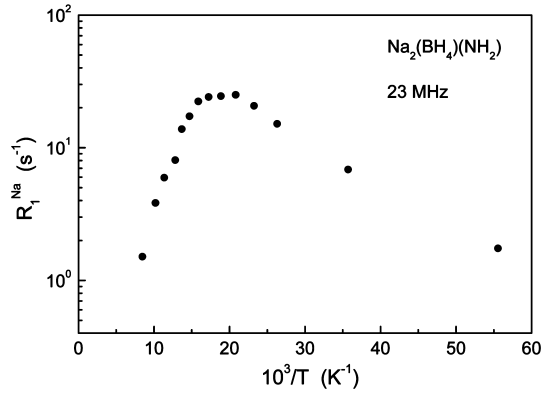

Figure 8. ^{23}Na spin−lattice relaxation rate measured at 23 MHz for $Na_2(BH_4)(NH_2)$ as a function of the inverse temperature. The data are shown in the temperature range 18−118 K.

measurements shown in Figure 8. Note that only the central ^{23}Na NMR line is excited in these experiments. The measured ^{23}Na spin−lattice relaxation rate R_1^{Na} exhibits the peak at nearly the same temperature as the $R_1^H(T)$ peak, and the general features of the temperature dependence of R_1^{Na} in the low-T region are similar to those of R_1^H (see Figure 5). It should be

dx.doi.org/10.1021/jp503451d | J. Phys. Chem. C 2014, 118, 14805−14812

noted that the amplitude of the observed $R_1^{Na}(T)$ peak is considerably higher than that expected for the $^{23}Na-^{1}H$ dipole−dipole interactions. The estimate of the maximum R_1^{Na} value due to the $^{23}Na-^{1}H$ dipole−dipole interactions modulated by reorientations of both BH_4 and NH_2 groups gives 1.9 s^{-1} at 23 MHz, whereas the observed maximum R_1^{Na} value is 25 s^{-1}. Thus, the dominant contribution to the ^{23}Na spin−lattice relaxation rate in the low-T region should originate from the quadrupole interaction modulated by anion reorientations.

High-Temperature Region. The behavior of the measured proton spin−lattice relaxation rates as functions of the inverse temperature in the region of the high-temperature peak is shown in Figure 9. For the previously studied borohydride-based systems, the high-temperature $R_1^H(T)$ peak was shown to originate from the translational diffusion of cations (as in the case of $LiBH_4$[22,32] and $LiBH_4$−LiI solid solutions[19]) or from the combined effect of the cation diffusion and a certain type of BH_4 reorientations occurring at the same frequency scale (as in the case of $LiLa(BH_4)_3Cl$[10]). For $Na_2(BH_4)(NH_2)$, the Na^+ jump rates appear to be too low to contribute to the observed high-temperature $R_1^H(T)$ peak; this is supported by the ^{23}Na spin−lattice relaxation measurements (to be discussed below). Therefore, the high-temperature $R_1^H(T)$ peak for $Na_2(BH_4)(NH_2)$ should be attributed to some reorientational process which is much slower than that responsible for the low-temperature $R_1^H(T)$ peak.

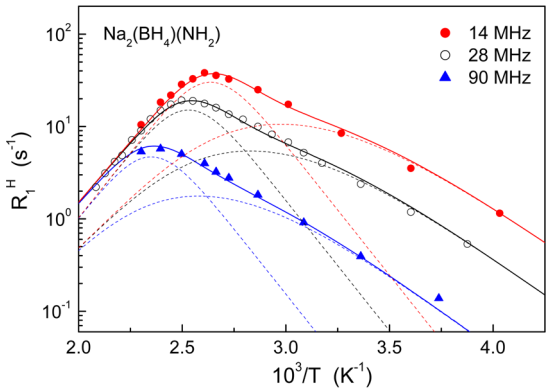

Figure 9. Proton spin−lattice relaxation rates measured at 14, 28, and 90 MHz for $Na_2(BH_4)(NH_2)$ as functions of the inverse temperature. The data are shown in the temperature range 248−480 K. The solid lines show the simultaneous fit of the two-peak model to the data. The dashed lines show the separate contributions of the faster and slower processes to the composite peak.

A coexistence of several reorientational processes with different characteristic jump rates have been reported earlier for a number of borohydrides.[10,19−21,24,28,31] The coexisting processes may originate from reorientations around different (inequivalent) symmetry axes of the BH_4 group.[24] A close inspection of the shape of the high-temperature $R_1^H(T)$ peak for $Na_2(BH_4)(NH_2)$ (Figure 9) shows that it should be described as a superposition of two partially overlapping peaks. We have found that it is impossible to provide a satisfactory description of both the temperature and frequency dependences of the proton spin−lattice relaxation rates in the high-T region in terms of a single peak. Thus, we have to assume the presence of at least two jump processes contributing to the observed behavior of R_1^H in the high-T region. It is evident that BH_4 groups are involved since the ^{11}B spin−lattice relaxation rate exhibits the peak at nearly the same temperature as the high-T peak of R_1^H (see Figure 6). Therefore, the two H jump processes may correspond to two types of BH_4 reorientations or to one type of BH_4 reorientation and one type of NH_2 reorientation. To the best of our knowledge, the only well-documented case of reorientational motion of NH_2 groups in amides is that of KNH_2.[41] The coordination of NH_2 groups in $Na_2(BH_4)(NH_2)$ differs from that in KNH_2. To reliably distinguish between the motion of BH_4 and NH_2 groups in $Na_2(BH_4)(NH_2)$, deuterium substitution in one of the groups would be desirable. The motional parameters of the two processes contributing to the high-T peak will be denoted by indices i = 2 (for the faster one) and 3 (for the slower one). The weak frequency dependence of R_1^H at the low-temperature slope (Figure 9) suggests the use of a distribution of activation energies for i = 2, while for i = 3 it is not necessary to use any distribution. Thus, for parametrization of the $R_1^H(T)$ data in the high-T region we shall use the two-peak model with a Gaussian distribution of the activation energies for one of the peaks; the parameters of this model are ΔM_2, τ_{02}, $\bar{E}_{a2}$, ΔE_{a2}, ΔM_3, τ_{03}, and E_{a3}. Other aspects of our approach are similar to those used for the low-T region. In particular, the description is based on analogues of eqs 1−3, and we look for the best fit of the model to the data at three resonance frequencies simultaneously. The solid lines in Figure 9 show the results of the simultaneous fit of this model to the $R_1^H(T)$ data at three resonance frequencies in the range 248−480 K. The dashed lines in this figure show the separate contributions of the faster process (i = 2) and the slower process (i = 3) to the composite peak. The amplitude parameters resulting from this fit are $\Delta M_2 = 4.9 \times 10^8$ s^{-2} and $\Delta M_3 = 9.1 \times 10^8$ s^{-2}, and the corresponding motional parameters are $\tau_{02} = (1.3 \pm 0.4) \times 10^{-14}$ s, $\bar{E}_{a2} = 340 \pm 9$ meV, $\Delta E_{a2} = 32 \pm 6$ meV, $\tau_{03} = (4.4 \pm 0.5) \times 10^{-16}$ s, and $E_{a3} = 559 \pm 7$ meV. Note that the value of E_{a3} appears to be the largest activation energy for reorientational motion in the studied borohydride-based systems. As mentioned above, we cannot exclude that one of the motional processes (i = 2, 3) is related to NH_2 reorientations.

In the high-temperature region, ^{23}Na NMR measurements at low magnetic field ($\omega/2\pi$ = 23 MHz) resulted in rather poor signal-to-noise ratios. Therefore, ^{23}Na NMR measurements in this region have been performed at the high magnetic field ($\omega/2\pi$ = 132.3 MHz). Figure 10 shows the evolution of the high-field ^{23}Na NMR spectrum for $Na_2(BH_4)(NH_2)$ with temperature.

The observed splitting of the low-temperature ^{23}Na NMR line at $\omega/2\pi$ = 132.3 MHz is nearly a factor of 132.3/23 = 5.75 smaller than the splitting at 23 MHz (see Figure 7). This is what is expected for the case of the second-order quadrupole splitting of the central NMR line.[40] With increasing temperature, the ^{23}Na NMR spectrum becomes narrower, and its shape exhibits peculiar changes. These changes are likely to originate from atomic motion in the system. In particular, the onset of such changes is expected to occur at the temperature at which the EFG fluctuation rate becomes comparable to the quadrupole frequency ν_Q. It should be noted that it is extremely difficult to simulate NMR line shapes in situations when a strong quadrupole interaction is partially averaged by atomic motion. Moreover, such a simulation would require detailed knowledge of the structure. For $Na_2(BH_4)(NH_2)$, the exact directions of the N−H bonds are not known.[15] Therefore, we have not tried to model the ^{23}Na spectra partially averaged by motion. Note that the ^{23}Na quadrupole interaction is not fully

dx.doi.org/10.1021/jp503451d | J. Phys. Chem. C 2014, 118, 14805−14812

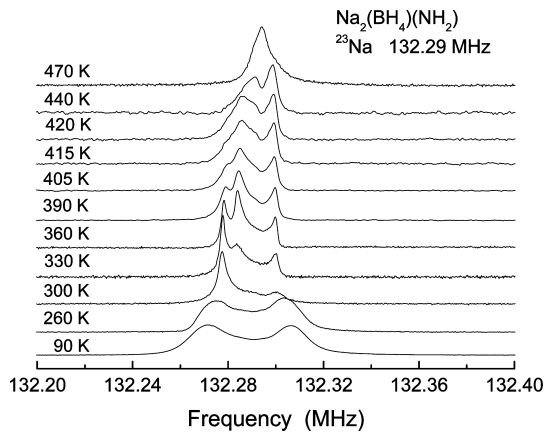

Figure 10. Evolution of the high-field ^{23}Na NMR spectrum for $Na_2(BH_4)(NH_2)$ with temperature.

averaged out even at 470 K. To find out whether the translational diffusion of Na^+ ions is observable at the NMR frequency scale, we have measured the temperature dependence of the ^{23}Na spin−lattice relaxation rate at $\omega/2\pi$ = 132.3 MHz and $T \geq 300$ K. The recovery of the ^{23}Na nuclear magnetization is well described by a single exponential function over the entire studied temperature range (300−470 K). The results of the ^{23}Na spin−lattice relaxation measurements are shown as an Arrhenius plot in Figure 11.

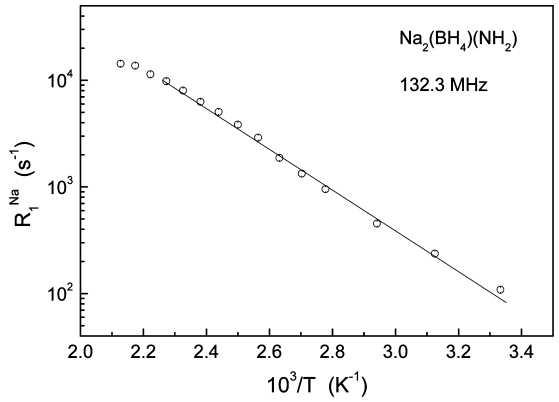

Figure 11. ^{23}Na spin−lattice relaxation rate measured at 132.3 MHz for $Na_2(BH_4)(NH_2)$ as a function of the inverse temperature. The data are shown in the temperature range 300−470 K. The solid line shows the Arrhenius fit to the data in the range 300−440 K.

As can be seen from this figure, the measured ^{23}Na spin−lattice relaxation rate R_1^{Na} strongly increases with increasing temperature. Thus, the behavior of R_1^{Na} in the high-temperature region differs from that of R_1^H (see Figure 9). Therefore, in contrast to $R_1^{Na}(T)$ in the low-temperature region, it cannot be related to anion reorientations. This suggests that in the high-T region $R_1^{Na}(T)$ is governed by translational diffusion of Na^+ ions, in qualitative agreement with the ionic conductivity measurements.[13] Such a conclusion is also supported by the strength of EFG fluctuations at ^{23}Na nuclei. Indeed, a comparison of Figures 11 and 8 shows that the values of R_1^{Na} in the high-T region are 2−3 orders of magnitude higher than those in the low-T region. If the R_1^{Na} measurements in the high-T and low-T regions were performed at the same resonance frequency, this difference would be even larger. It should be noted that the "ideal" reorientations of BH_4 or NH_2 groups are not expected to lead to any EFG fluctuations at Na sites since the charge distribution remains the same after a reorientational jump. This reflects the fundamental difference between the dipole−dipole and quadrupole interactions. While the dipole−dipole interaction is *pairwise* (and, thus, depends on orientations of the vectors connecting each pair), the nuclear quadrupole moment interacts with the entire charge distribution. This means that EFG fluctuations at Na sites could be related only to deviations from the "ideal" reorientations. The corresponding contribution to the ^{23}Na spin−lattice relaxation rate is relatively weak, as reflected by the R_1^{Na} data in the low-T region. On the other hand, Na^+ jumps can strongly contribute to the measured quadrupolar ^{23}Na spin−lattice relaxation rate if each jump changes the direction of the principal axis of the EFG at Na sites. The axial symmetry of Na sites in $Na_2(BH_4)(NH_2)$ (Figure 2) suggests that Na^+ jumps between the nearest-neighbor sites should be accompanied by $\pi/2$ rotations of the EFG axes. Taking into account the large value of ν_Q for ^{23}Na in $Na_2(BH_4)(NH_2)$ (see above), we conclude that the diffusive jumps of Na^+ ions provide a strong relaxation mechanism for ^{23}Na in this compound. However, since the ^{1}H−^{23}Na dipole−dipole interaction is weak (as compared to the ^{1}H−^{1}H and ^{1}H−^{11}B dipolar interactions), the diffusive Na^+ jumps only slightly affect the ^{1}H spin−lattice relaxation rate.

As can be seen from Figure 11, the temperature dependence of R_1^{Na} is satisfactorily described by the Arrhenius law over the range of 300−440 K and shows some signs of saturation above 440 K. This indicates that, with increasing temperature, the "slow-motion" regime (for which the diffusive jump rate τ_d^{-1} is much lower than the resonance frequency ω_{Na} and R_1^{Na} is proportional to τ_d^{-1}) starts to transform into an "intermediate-motion" regime (for which τ_d^{-1} becomes comparable to ω_{Na} and R_1^{Na} approaches its maximum). The solid line in Figure 11 represents the Arrhenius fit to the data in the range 300−440 K. In this range, the measured ^{23}Na relaxation rate is expected to be proportional to τ_d^{-1}. The activation energy for the diffusive motion, E_a^d, derived from this fit is 380 ± 10 meV. This value appears to be rather low for ionic diffusion. However, since the relaxation rate maximum related to this motional process is not reached in our experiments, this value of the activation energy should be considered only as a rough estimate; moreover, we cannot determine the absolute values of τ_d^{-1}. We can only state that at 470 K (the highest temperature of our measurements

Table 1. Activation Energies for Different Types of Atomic Motion in $Na_2(BH_4)(NH_2)$ Derived from NMR Measurements[a]

type of motion	jump rate parameter	T range (K)	average activation energy (meV)	activation energy dispersion (meV)
reorientational H jumps	τ_1^{-1}	13−190	74(7)	29(5)
reorientational H jumps	τ_2^{-1}	248−480	340(9)	32(6)
reorientational H jumps	τ_3^{-1}	248−480	559(7)	-
diffusive Na jumps	τ_d^{-1}	300−440	380(10)	-

[a]Uncertainties in the last digit are given in parentheses.

dx.doi.org/10.1021/jp503451d | J. Phys. Chem. C 2014, 118, 14805−14812

which is close to the melting point of 492 K[15]) the jump rate τ_d^{-1} remains below $\omega \approx 8 \times 10^8$ s^{-1}. The activation energy derived from the conductivity data[13] for $Na_2(BH_4)(NH_2)$ in the range 300−423 K is 0.61(1) eV.

The activation energies for different types of atomic motion in $Na_2(BH_4)(NH_2)$ obtained from our NMR data are summarized in Table 1.

This table shows that the spectrum of various atomic motions in the sodium borohydride−amide is very broad. For the reorientational motion characterized by the jump rate τ_1^{-1} the activation energy is small; this fast motion provides the dominant contribution to the measured spin−lattice relaxation rates in the low-temperature region. The slower reorientational motions with the jump rates τ_2^{-1} and τ_3^{-1} are characterized by much higher activation energies; these motions provide the dominant contributions to the proton spin−lattice relaxation rate in the region of the high-temperature peak. The diffusive motion of Na^+ ions is observable at the NMR frequency scale; however, the corresponding ^{23}Na relaxation rate maximum is not reached up to 470 K. This means that, in contrast to the case of $LiLa(BH_4)_3Cl$,[10] for $Na_2(BH_4)(NH_2)$ the cation diffusive jumps and the slower anion reorientations do not occur at the same frequency scale.

CONCLUSIONS

The analysis of the temperature and frequency dependences of the measured proton spin−lattice relaxation rate for $Na_2(BH_4)(NH_2)$ has revealed at least three reorientational jump processes in this mixed borohydride−amide. For the fastest reorientational jump process, the most probable value of the jump rate is found to reach ~10^8 s^{-1} at 70 K. Our ^{1}H spin−lattice relaxation rate results in the low-temperature region (13−190 K) are satisfactorily described by a Gaussian distribution of the activation energies with the average E_a value of 74 meV. Above 200 K, this reorientational jump process becomes too fast to be probed by NMR. Our ^{1}H spin−lattice relaxation data in the high-temperature region (250−480 K) are governed by two other (slower) jump processes characterized by the average activation energies of 340 and 559 meV. Both these processes correspond to reorientational motion; however, their exact nature is not yet clear. One of the possibilities is that they are associated with specific reorientations of BH_4 and NH_2 groups. The geometry of these reorientations could, in principle, be clarified by quasielastic neutron scattering measurements. Up to the temperatures close to the melting point of $Na_2(BH_4)(NH_2)$, we have not found any signs of translational diffusion of H-containing species at the frequency scale of 10^5 s^{-1} or higher. The ^{23}Na spin−lattice relaxation data in the high-temperature region are governed by translational diffusion of Na^+ ions, which is consistent with the ionic conductivity measurements[13] for $Na_2(BH_4)(NH_2)$.

AUTHOR INFORMATION

Corresponding Author

*E-mail: skripov@imp.uran.ru. Fax: +7-343-374-5244.

Notes

The authors declare no competing financial interest.

ACKNOWLEDGMENTS

This work was partially supported by the Russian Foundation for Basic Research (Grant No. 12-03-00078) and by the Priority Program "Physico-technical principles of development of technologies and devices for smart adaptive electrical networks" of the Russian Academy of Sciences. The authors also acknowledge financial support from the Integrated Materials Research Center for the Low-Carbon Society (LC-IMR), Tohoku University, and JSPS KAKENHI Grant No. 25220911.

REFERENCES

(1) Orimo, S.; Nakamori, Y.; Elisen, J. R.; Züttel, A.; Jensen, C. M. Complex Hydrides for Hydrogen Storage. *Chem. Rev.* **2007**, *107*, 4111−4132.

(2) Matsuo, M.; Nakamori, Y.; Orimo, S.; Maekawa, H.; Takamura, H. Lithium Superionic Conduction in Lithium Borohydride Accompanied by Structural Transition. *Appl. Phys. Lett.* **2007**, *91*, 224103.

(3) Maekawa, H.; Matsuo, M.; Takamura, H.; Ando, M.; Noda, Y.; Karahashi, T.; Orimo, S. Halide-Stabilized $LiBH_4$, a Room-Temperature Lithium Fast-Ion Conductor. *J. Am. Chem. Soc.* **2009**, *131*, 894−895.

(4) Matsuo, M.; Takamura, H.; Maekawa, H.; Li, H.-W.; Orimo, S. Stabilization of Lithium Superionic Conduction Phase and Enhancement of Conductivity of $LiBH_4$ by LiCl Addition. *Appl. Phys. Lett.* **2009**, *94*, 084103.

(5) Miyazaki, R.; Karahashi, T.; Kamatani, N.; Noda, Y.; Ando, M.; Takamura, H.; Matsuo, M.; Orimo, S.; Maekawa, H. Room Temperature Lithium Fast-Ion Conduction and Phase Relashionship in LiI Stabilized $LiBH_4$. *Solid State Ionics* **2011**, *192*, 143−147.

(6) Matsuo, M.; Remhof, A.; Martelli, P.; Caputo, R.; Ernst, M.; Miura, Y.; Sato, T.; Oguchi, H.; Maekawa, H.; Takamura, H.; Borgschulte, A.; Züttel, A.; Orimo, S. Complex Hydrides with $(BH_4)^-$ and $(NH_2)^-$ Anions as New Lithium Fast-Ion Conductors. *J. Am. Chem. Soc.* **2009**, *131*, 16389−16391.

(7) Matsuo, M.; Sato, T.; Miura, Y.; Oguchi, H.; Zhou, Y.; Maekawa, H.; Takamura, H.; Orimo, S. Synthesis and Lithium Fast-Ion Conductivity of a New Complex Hydride $Li_3(NH_2)_2I$ with Double-Layered Structure. *Chem. Mater.* **2010**, *22*, 2702−2704.

(8) Ley, M. B.; Ravnsbæk, D. B.; Filinchuk, Y.; Lee, Y. S.; Janot, R.; Cho, Y. W.; Skibsted, J.; Jensen, T. R. $LiCe(BH_4)_3Cl$, a New Lithium-Ion Conductor and Hydrogen Storage Material with Isolated Tetranuclear Anionic Clusters. *Chem. Mater.* **2012**, *24*, 1654−1663.

(9) Ley, M. B.; Boulineau, S.; Janot, R.; Filinchuk, Y.; Jensen, T. R. New Li Ion Conductors and Solid State Hydrogen Storage Materials: $LiM(BH_4)_3Cl$, M = La, Gd. *J. Phys. Chem. C* **2012**, *116*, 21267−21276.

(10) Skripov, A. V.; Soloninin, A. V.; Ley, M. B.; Jensen, T. R.; Filinchuk, Y. Nuclear Magnetic Resonance Studies of BH_4 Reorientations and Li Diffusion in $LiLa(BH_4)_3Cl$. *J. Phys. Chem. C* **2013**, *117*, 14965−14972.

(11) Udovic, T. J.; Matsuo, M.; Unemoto, A.; Verdal, N.; Stavila, V.; Skripov, A. V.; Rush, J. J.; Takamura, H.; Orimo, S. Sodium Superionic Conduction in $Na_2B_{12}H_{12}$. *Chem. Commun.* **2014**, *50*, 3750−3752.

(12) Skripov, A. V.; Babanova, O. A.; Soloninin, A. V.; Stavila, V.; Verdal, N.; Udovic, T. J.; Rush, J. J. Nuclear Magnetic Resonance Study of Atomic Motion in $A_2B_{12}H_{12}$ (A = Na, K, Rb, Cs): Anion Reorientations and Na^+ Mobility. *J. Phys. Chem. C* **2013**, *117*, 25961−25968.

(13) Matsuo, M.; Kuromoto, S.; Sato, S.; Oguchi, H.; Takamuro, H.; Orimo, S. Sodium Ionic Conduction in Complex Hydrides with $[BH_4]^-$ and $[NH_2]^-$ Anions. *Appl. Phys. Lett.* **2012**, *100*, 203904.

(14) Chater, P. A.; Anderson, P. A.; Prendergast, J. W.; Walton, A.; Mann, V. S. J.; Book, D.; David, W. I. F.; Johnson, S. R.; Edwards, P. P. Synthesis and Characterization of Amide-Borohydrides: New Complex Light Hydrides for Potential Hydrogen Storage. *J. Alloys Compd.* **2007**, *446−447*, 350−354.

(15) Somer, M.; Acar, S.; Koz, C.; Kokal, I.; Höhn, P.; Cardoso-Gil, R.; Aydemir, U.; Akselrud, L. α- and β-$Na_2[BH_4][NH_2]$: Two Modifications of a Complex Hydride in the System $NaNH_2$-$NaBH_4$;

Syntheses, Crystal Structures, Thermal Analyses, Mass and Vibrational Spectra. *J. Alloys Compd.* **2010**, *491*, 98−105.
(16) Remhof, A.; Łodziana, Z.; Martelli, P.; Friedrichs, O.; Züttel, A.; Skripov, A. V.; Embs, J. P.; Strässle, T. Rotational Motion of BH_4 Units in MBH_4 (M = Li, Na, K) from Quasielastic Neutron Scattering and Density Functional Calculations. *Phys. Rev. B* **2010**, *81*, 214304.
(17) Verdal, N.; Udovic, T. J.; Rush, J. J. The Nature of BH_4 Reorientations in Hexagonal $LiBH_4$. *J. Phys. Chem. C* **2012**, *116*, 1614−1618.
(18) Martelli, P.; Remhof, A.; Borgschulte, A.; Ackermann, R.; Strässle, T.; Embs, J. P.; Ernst, M.; Matsuo, M.; Orimo, S.; Züttel, A. Rotational Motion in $LiBH_4$/LiI Solid Solutions. *J. Phys. Chem. A* **2011**, *115*, 5329−5334.
(19) Skripov, A. V.; Soloninin, A. V.; Rude, L. H.; Jensen, T. R.; Filinchuk, Y. Nuclear Magnetic Resonance Studies of Reorientational Motion and Li Diffusion in $LiBH_4$-LiI Solid Solutions. *J. Phys. Chem. C* **2012**, *116*, 26177−26184.
(20) Verdal, N.; Udovic, T. J.; Rush, J. J.; Wu, H.; Skripov, A. V. Evolution of the Reorientational Motions of the Tetrahydroborate Anions in Hexagonal $LiBH_4$-LiI Solid Solution by High-Q Quasielastic Neutron Scattering. *J. Phys. Chem. C* **2013**, *117*, 12010−12018.
(21) Skripov, A. V.; Soloninin, A. V.; Filinchuk, Y.; Chernyshov, D. Nuclear Magnetic Resonance Study of the Rotational Motion and the Phase Transition in $LiBH_4$. *J. Phys. Chem. C* **2008**, *112*, 18701−18705.
(22) Corey, R. L.; Shane, D. T.; Bowman, R. C.; Conradi, M. S. Atomic Motions in $LiBH_4$ by NMR. *J. Phys. Chem. C* **2008**, *112*, 18706−18710.
(23) Babanova, O. A.; Soloninin, A. V.; Stepanov, A. P.; Skripov, A. V.; Filinchuk, Y. Structural and Dynamical Properties of $NaBH_4$ and KBH_4: NMR and Synchrotron X-ray Diffraction Studies. *J. Phys. Chem. C* **2010**, *114*, 3712−3718.
(24) Skripov, A. V.; Soloninin, A. V.; Babanova, O. A.; Hagemann, H.; Filinchuk, Y. Nuclear Magnetic Resonance Study of Reorientational Motion in α-$Mg(BH_4)_2$. *J. Phys. Chem. C* **2010**, *114*, 12370−12374.
(25) Shane, D. T.; Corey, R. L.; McIntosh, C.; Rayhel, L. H.; Bowman, R. C.; Vajo, J. J.; Gross, A. F.; Conradi, M. S. $LiBH_4$ in Carbon Aerogel Nanoscaffolds: An NMR Study of Atomic Motions. *J. Phys. Chem. C* **2010**, *114*, 4008−4014.
(26) Babanova, O. A.; Soloninin, A. V.; Skripov, A. V.; Ravnsbæk, D. B.; Jensen, T. R.; Filinchuk, Y. Reorientational Motion in Alkali-Metal Borohydrides: NMR Data for $RbBH_4$ and $CsBH_4$ and Systematics of the Activation Energy Variations. *J. Phys. Chem. C* **2011**, *115*, 10305−10309.
(27) Shane, D. T.; Rayhel, L. H.; Huang, Z.; Zhao, J. C.; Tang, X.; Stavila, V.; Conradi, M. S. Comprehensive NMR Study of Magnesium Borohydride. *J. Phys. Chem. C* **2011**, *115*, 3172−3177.
(28) Soloninin, A. V.; Babanova, O. A.; Skripov, A. V.; Hagemann, H.; Richter, B.; Jensen, T. R.; Filinchuk, Y. NMR Study of Reorientational Motion in Alkaline-Earth Borohydrides: β and γ Phases of $Mg(BH_4)_2$ and α and β Phases of $Ca(BH_4)_2$. *J. Phys. Chem. C* **2012**, *116*, 4913−4920.
(29) Jimura, K.; Hayashi, S. Reorientational Motion of BH_4 Ions in Alkali Borohydrides MBH_4 (M = Li, Na, K) As Studied by Solid-State NMR. *J. Phys. Chem. C* **2012**, *116*, 4883−4891.
(30) Eagles, M.; Sun, B.; Richter, B.; Jensen, T. R.; Filinchuk, Y.; Conradi, M. S. NMR Investigation of Nanoporous γ-$Mg(BH_4)_2$ and Its Thermally Induced Phase Changes. *J. Phys. Chem. C* **2012**, *116*, 13033−13037.
(31) Soloninin, A. V.; Skripov, A. V.; Yan, Y.; Remhof, A. Nuclear Magnetic Resonance Study of Hydrogen Dynamics in $Y(BH_4)_3$. *J. Alloys Compd.* **2013**, *555*, 209−212.
(32) Soloninin, A. V.; Skripov, A. V.; Buzlukov, A. L.; Stepanov, A. P. Nuclear Magnetic Resonance Study of Li and H Diffusion in the High-Temperature Solid Phase of $LiBH_4$. *J. Solid State Chem.* **2009**, *182*, 2357−2361.
(33) Epp, V.; Wilkening, M. Fast Li Diffusion in Crystalline $LiBH_4$ Due to Reduced Dimensionality: Frequency-Dependent NMR Spectroscopy. *Phys. Rev. B* **2010**, *82*, 020301(R).
(34) Fukushima, E.; Roeder, S. B. W. *Experimental Pulse NMR: a Nuts and Bolts Approach*; Addison-Wesley: Reading, 1981.
(35) Clark, W. G. Pulsed Nuclear Magnetic Resonance Apparatus. *Rev. Sci. Instrum.* **1964**, *35*, 316−333.
(36) Avogadro, A.; Bonera, G.; Villa, M. The Clark Method of Recording Lineshapes. *J. Magn. Reson.* **1979**, *35*, 387−407.
(37) Abragam, A. *The Principles of Nuclear Magnetism*; Clarendon Press: Oxford, 1961.
(38) Sorte, E. G.; Emery, S. B.; Majzoub, E. H.; Ellis-Caleo, T.; Ma, Z. L.; Hammann, B. A.; Hayes, S. E.; Bowman, R. C.; Conradi, M. S. NMR Study of Anion Dynamics in Solid $KAlH_4$. *J. Phys. Chem. C* **2014**, *118*, 5725−5732.
(39) Markert, J. T.; Cotts, E. J.; Cotts, R. M. Hydrogen Diffusion in the Metallic Glass a-$Zr_3RhH_{3.5}$. *Phys. Rev. B* **1988**, *37*, 6446−6452.
(40) Cohen, M. H.; Reif, F. Quadrupole Effects in Nuclear Magnetic Resonance Studies of Solids. In *Solid State Physics*; Seitz, F., Turnbull, D., Eds.; Academic Press: New York, 1957; Vol. *5*, pp 321−438.
(41) Müller, M.; Asmussen, B.; Press, W.; Senker, J.; Jacobs, H.; Büttner, H.; Schober, H. Orientational Order and Rotational Dynamics of the Amide Ions in Potassium Amide. II. Quasielastic Neutron Scattering. *J. Chem. Phys.* **1998**, *109*, 3559−3567.